Electronic Supplementary Information

Large heterometallic coordination cages with gyrobifastigium-like geometry

Giacomo Cecot,[a] Bassam Alameddine,[b] Stéphanie Prior,[a] Rita De Zorzi,[c] Silvano Geremia,[c] Rosario Scopelliti,[a] Fadaei T. Farzaneh,[a] Euro Solari,[a] and Kay Severin*[a]

[a] *Institut des Sciences et Ingénierie Chimiques, École Polytechnique Fédérale de Lausanne (EPFL), 1015 Lausanne, Switzerland*
[b] *Department of Mathematics and Natural Sciences, Gulf University of Science & Technology (GUST), Kuwait*
[c] *Centro di Eccellenza in Biocristallografia, Dipartimento di Science Chimiche e Farmaceutiche, Università di Trieste, Trieste, Italy*
* *E-mail: kay.severin@epfl.ch.*

Table of contents:

1. General

Chemicals were obtained from commercial sources (see below) and used without further purification unless stated otherwise. Diethyl glyoxime[1] was prepared as described in the literature along with (dppp)$PtCl_2$,[2] (dppp)$Pt(OTf)_2$,[3] (dppp)$PdCl_2$,[4] (dppp)$Pd(OTf)_2$[3] and (dppm)$PtCl_2$.[2] Complex (dppm)$Pt(OTf)_2$ was prepared in analogy to the procedure used for (dppp)$Pt(OTf)_2$.[3] All reactions were performed under an atmosphere of nitrogen using standard Schlenk techniques. All solvents were degassed before being used.

Commercial sources: 3,5-Dibromophenylboronic acid – Fluorochem, anhydrous iron(II) chloride – Acros, dimethylglyoxime – Apollo Scientific, pyridine-4-boronic acid hydrate – Fluorochem, S-PHOS – ABCR, tris(dibenzylideneacetone)dipalladium(0) – ABCR, K_3PO_4 – Acros, K_2PtCl_4 – Precious metal online, Na_2PdCl_4 – Precious metal online, bis(diphenylphosphino)methane – ABCR, 1,3-bis(diphenylphosphino)propane – Fluorochem, silver trifluoromethanesulfonate – Fluorochem.

NMR spectra were obtained on a Bruker Avance III spectrometer (^{1}H: 400 MHz) or a Bruker Avance III HD spectrometer (^{1}H: 600MHz) The chemical shifts are reported in parts per million δ (ppm) referenced to the residual solvent signal. All spectra were recorded at 298 K. ^{31}P spectra are referenced to an external standard (H_3PO_4 85%). The analysis of the NMR spectra were performed with MestreNova. For the DOSY analysis, the Baysian DOSY transform from MestreNova was employed.

High resolution mass spectra of the clathrochelates **1**−**4** were obtained using a Xevo G2-S QTOF mass spectrometer coupled to the Acquity UPLC Class Binary Solvent manager and BTN sample manager (Waters, Corporation, Milford, MA). The sample manager system temperature was maintained at 10 °C and the injection volume was 2 μL. Mass spectrometer detection was operated in positive ionization using the ZSpray™ dual-orthogonal multimode ESI/APCI/ESCi® source. The TOF mass spectra were acquired in the resolution mode over the range of m/z 50−1200 at an acquisition rate of 0.036 sec/spectra. Source settings were as follows: cone, 25V; capillary, 3 kV, source temperature, 150°C; desolvation temperature, 500°C, cone gas, 10 L/h, desolvation gas, 500 L/h. Data were processed using MassLynx™ 4.1 software.

High resolution mass spectra of the cages **5**−**7** were obtained as follows: The analytes were dissolved in acetonitrile to a final concentration of ~10−30 μM. The experiments were carried out using a LTQ Orbitrap FTMS instrument (LTQ Orbitrap Elite FTMS, Thermo Scientific, Bremen, Germany) operated in the positive mode coupled with a robotic chip-based nano-ESI source (TriVersa Nanomate, Advion Biosciences, Ithaca, NY, U.S.A.). To reduce the degree of analyte gas phase reactions leading to side products unrelated to solution phase, the transfer capillary temperature was lowered to 80 °C. A standard data acquisition and instrument control system was utilized (Thermo Scientific) whereas the ion source was controlled by Chipsoft 8.3.1 software (Advion BioScience). Samples were loaded onto a 96-well plate (Eppendorf, Hamburg, Germany) within an injection volume of 5μl. The experimental conditions for the ionization voltage was +1.4kV and the gas pressure was set at 0.30 psi. The temperature of ion transfer capillary was 80 °C, tube voltages. FTMS spectra were obtained in the 250−3000 *m/z* range in the reduce profile mode with a resolution set to 120,000. In all spectra, one microscan was acquired with a maximum injection time value of 1000ms. Post-acquisition analysis was performed using the ChemCalc (http://www.chemcalc.org/) web tool.[5]

2. Synthetic procedures

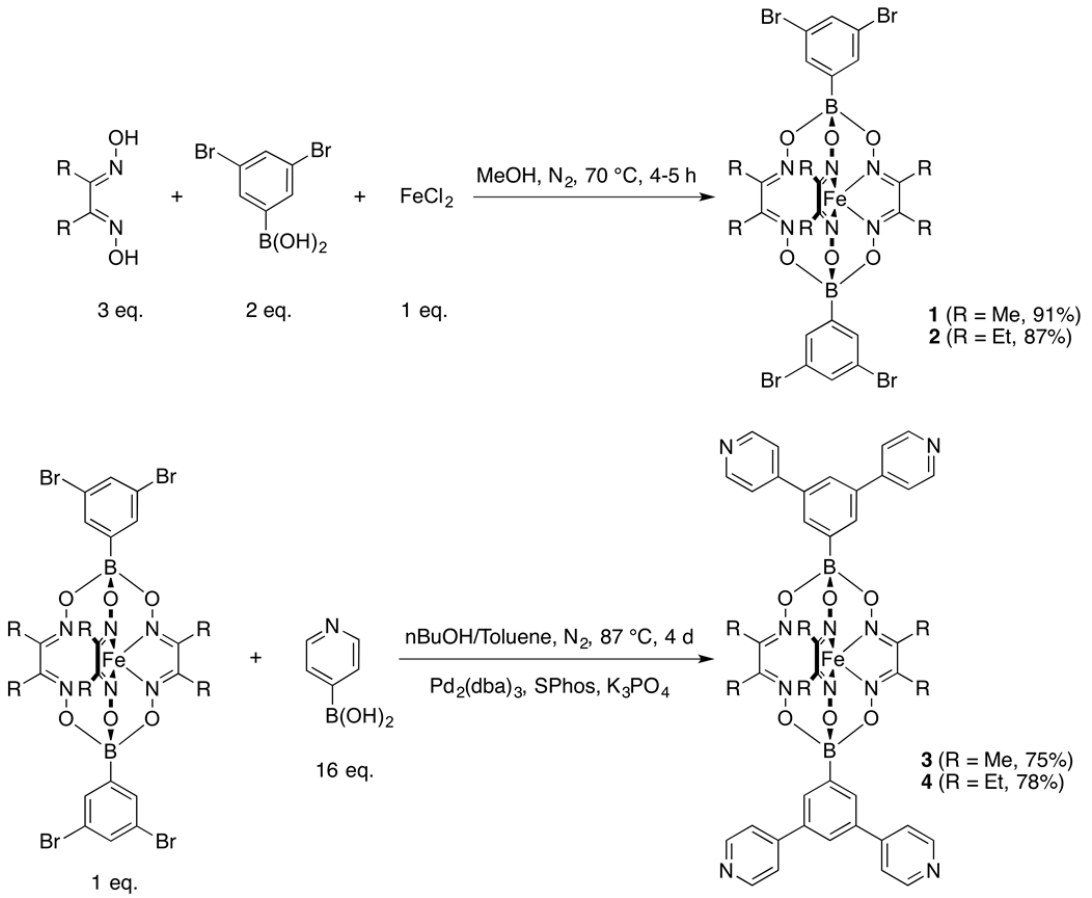

Scheme S1. Synthesis of the clathrochelate complexes **1**−**4**.

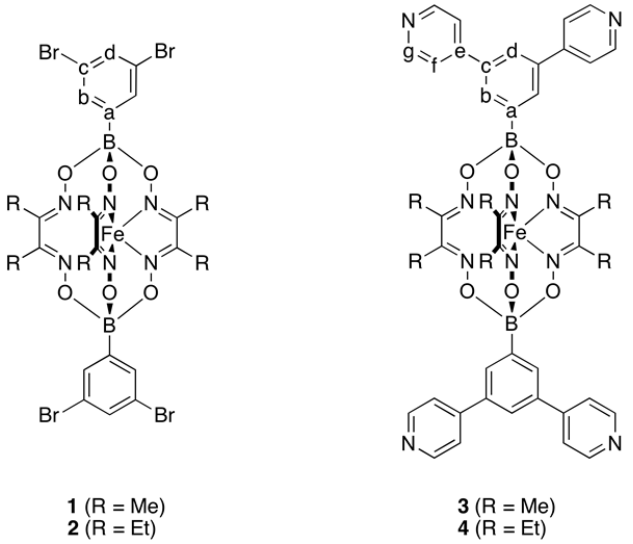

1 (R = Me)
2 (R = Et)

3 (R = Me)
4 (R = Et)

Scheme S2. Labelling for the assignment of thr NMR signals.

Clathrochelate 1

MeOH (20 mL) was added to a mixture of dimethylglyoxime (352 mg, 2.44 mmol), 3,5-dibromophenylboronic acid (461 mg, 1.65 mmol) and anhydrous $FeCl_2$ (103 mg, 0.82 mmol) leading to a red/orange suspension. The mixture was heated under reflux for 4 h and then it was allowed to cool to RT. The solvent was removed under reduced pressure and the mixture was then suspended in fresh MeOH (30 mL). The product was isolated by filtration, washed with MeOH (5 × 2 mL), DCM (few drops), Et_2O (5 × 2 mL), and pentane (5 × 2 mL) to give clathrochelate **1** in the form of a red powder (663 mg, 0.75 mmol, 91%).

^{1}H NMR (400 MHz, CD_2Cl_2) δ 7.74 (d, J = 1.9 Hz, 4 H, H_b), 7.64 (t, J = 1.9 Hz, 2 H, H_d), 2.42 (s, 18H, CH_3). ^{13}C NMR (151 MHz, CD_2Cl_2) δ 153.35 (C=N), 133.79 (C_b), 133.60 (C_d), 123.07 (C_c), 13.81 (CH_3) (C-B not detected). HRMS (ESI-QTOF): *m/z* calculated for $C_{24}H_{24}B_2Br_4FeN_6O_6$ $[M]^-$ 885.8031, found 885.7971.

Clathrochelate 2

MeOH (10 mL) was added to a mixture of diethylglyoxime (173 mg, 1.20 mmol), 3,5-dibromophenylboronic acid (224 mg, 0.80 mmol) and anhydrous $FeCl_2$ (50 mg, 0.40 mmol) leading to a red/orange suspension. The mixture was heated under reflux for 5 h and then it was allowed to cool to RT. The product was isolated by filtration, washed with MeOH (5 × 2 ml), DCM (few drops), Et_2O (5 × 2 ml), pentane (5 × 2 ml) to give clathrochelate **2** in the form of a red powder (343 mg, 0.35 mmol, 87%).

^{1}H NMR (400 MHz, $C_2D_2Cl_4$) δ 7.75 (s, 4 H, H_b), 7.66 (s, 2 H, H_d), 2.83 (q, J = 7.5 Hz, 12H, CH_2CH_3), 1.17 (t, J = 7.5 Hz, 18H, CH_2CH_3). Because of the poor solubility of **2**, a ^{13}C NMR spectrum was not recorded. HRMS (ESI): *m/z* calculated for $C_{30}H_{36}B_2Br_4FeN_6O_6$ $[M+H]^+$ 970.9043, found 970.9060.

Clathrochelate 3

A mixture of *n*BuOH and toluene (1:1, 30 mL) was added to a mixture of clathrochelate **1** (250 mg, 0.28 mmol), 4-pyridylboronic acid (658 mg, 4.67 mmol), $Pd_2(dba)_3$ (51 mg, 0.06 mmol), SPhos (47 mg, 0.12 mmol) and K_3PO_4 (487 mg, 2.29 mmol). The reaction mixture was stirred at 87 °C for 4 days and then it was allowed to cool to RT. The solvent was co-evaporated four times adding at each evaporation step toluene (100 mL). The resulting dark red powder was dissolved in DCM (80 mL) and transferred into a separation funnel. The organic layer was washed with a solution of saturated $NaHCO_3$ (1 × 250 mL), H_2O (3 × 150 mL) and dried over $MgSO_4$. After filtration, the solvent was removed under reduced pressure leading to a red powder. The product was purified via gradient column chromatography (SiO_2 230-400 mesh, 25 cm, ∅ 4 cm) DCM→DCM/MeOH 9:1. The fractions containing the product were collected and the solvent was removed under reduced pressure. The product was redissolved in a minimum amount of DCM and precipitated with Et_2O. The solid was isolated by filtration and washed with pentane (3 × 5 mL) to give clathrochelate **3** in the form of an orange powder (188 mg, 0.21 mmol, 75%).

^{1}H NMR (400 MHz, CD_2Cl_2) δ 8.68 (d, J = 6.1 Hz, 8 H, H_g), 8.10 (s, 4 H, H_b), 7.90 (s, 2 H, H_d), 7.65 (d, J = 6.2 Hz, 8 H, H_f), 2.47 (s, 18H, CH_3). ^{13}C NMR (151 MHz, CD_2Cl_2) δ 153.18 (C=N), 150.84 (C_g), 149.23 (C_c), 138.65 (C_e), 131.67 (C_b), 125.79 (C_d), 122.38 (C_f), 13.87 (CH_3), (C-B not detected). HRMS (ESI-QTOF): *m/z* calculated for $C_{44}H_{40}B_2FeN_{10}O_6$ $[M+H]^+$ 883.2746 and $[M+2H]^{2+}$ 442.1407, found 883.2761 and 442.1420.

Clathrochelate 4

A mixture of *n*BuOH and toluene (1:1, 15 mL) was added to a mixture of clathrochelate **2** (150 mg, 0.15 mmol), 4-pyridylboronic acid (347 mg, 2.46 mmol), $Pd_2(dba)_3$ (29 mg, 0.03 mmol), SPhos (26 mg, 0.06 mmol) and K_3PO_4 (263 mg, 1.24 mmol. The reaction mixture was stirred at 87 °C for 4 days and then it was allowed to cool to RT. The solvent was co-evaporated five times adding at each evaporation step toluene (50 mL). The resulting dark red powder was dissolved in DCM (40 mL) and transferred into a separation funnel. The organic layer was washed with a solution of saturated $NaHCO_3$ (1 × 150 mL), H_2O (3 × 150 mL) and dried over $MgSO_4$. After filtration, the solvent was removed under reduced pressure leading to an orange powder. The product was purified via gradient column chromatography (SiO_2 230-400 mesh, 40 cm, ∅ 4 cm) DCM→DCM/MeOH 9:1. The fractions containing the product were collected and the solvent was removed under reduced pressure. The product was re-dissolved in a minimum amount of DCM and precipitated with pentane (50 mL). The solid was isolated by filtration and washed with pentane (3 × 10 mL) to give clathrochelate **4** in the form of a orange powder (116 mg, 0.12 mmol, 78%).

^{1}H NMR (400 MHz, CD_2Cl_2) δ 8.68 (d, J = 6.1 Hz, 8 H, H_g), 8.11 (s, 4 H, H_b), 7.91 (s, 2 H, H_d), 7.64 (d, J = 6.1 Hz, 8 H, H_f), 2.89 (q, J = 7.5 Hz, 12H, CH_2CH_3), 1.23 (t, J = 7.5 Hz, 18H, CH_2CH_3). ^{13}C NMR (101 MHz, CD_2Cl_2) δ 158.77 (C=N), 150.86 (C_g), 149.27 (C_c), 138.63 (C_e), 131.66 (C_b), 125.67 (C_d), 122.33 (C_f), 21.51 (CH_2CH_3), 11.85 (CH_2CH_3) (C-B not detected). HRMS (ESI): *m/z* calculated for $C_{50}H_{52}B_2FeN_{10}O_6$ $[M+H]^+$ 967.3680, found 967.3685.

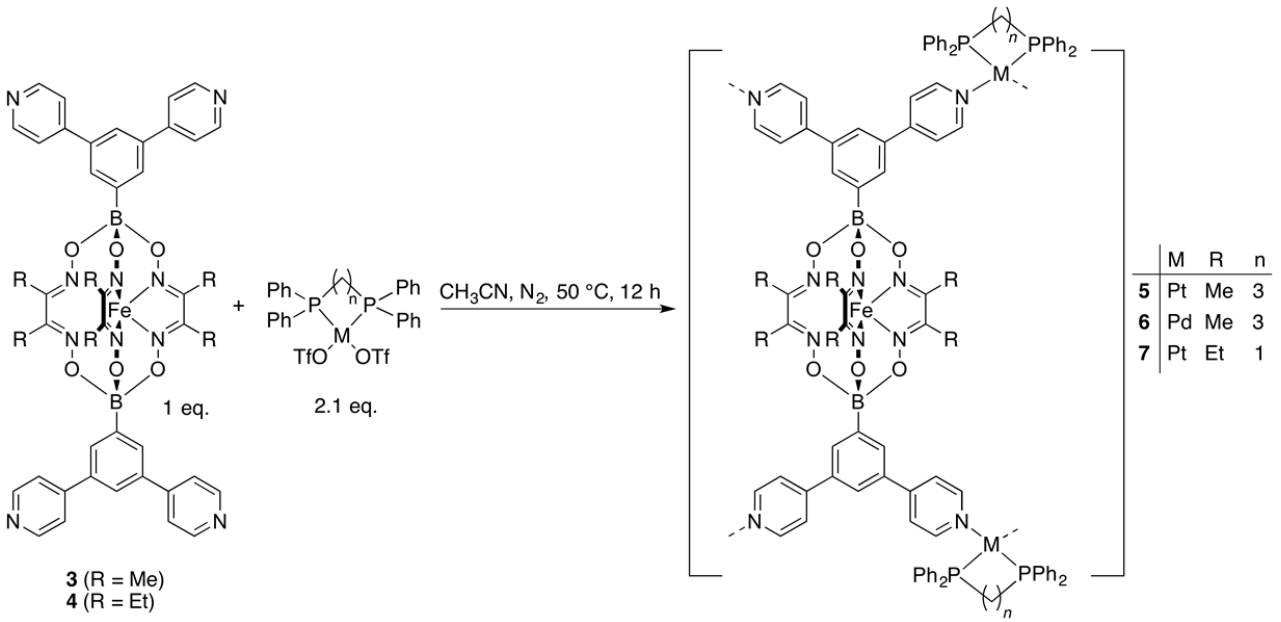

Scheme S3. Synthesis of the cages **5**−**7**.

Cage 5

Clathrochelate **3** (8.97 mg, 10 μmol) and (dppp)Pt(OTf)$_2$ (19.34 mg, 21 μmol) were suspended in CH_3CN (2.1 mL) and the reaction mixture was stirred at 50 °C over night. The solution became clear after approximately 1 h. The solution was filtered using *Whatman* glass filters and the product was precipitated with Et_2O (20 mL). The product was isolated by filtration, washed with Et_2O (1 × 5mL), pentane (3 × 5mL) and dried under vacuum to give **5** in the form of an orange powder (25.9 mg, 2.4 μmol, 96%).

^{1}H NMR (400 MHz, CD_3CN) δ 8.73 (broad d, J = 8.3 Hz, 32H, CH_{ar}), 7.83 (broad m, 24H, CH_{ar}), 7.79 (s, 8H, CH_{ar}), 7.70 (broad m, 32H, CH_{ar}), 7.63−7.30 (m, 152H) (CH_{ar}), 3.30 (broad m, 32H, PCH_2), 2.35 (broad m, 16H, PCH_2CH_2), 2.08 (s, 72H, CH_3). Because of the poor solubility of **5**, a ^{13}C NMR spectrum was not recorded.^{31}P NMR (162 MHz, CD_3CN) δ –13.00 (s), –13.15 (s), ^{195}Pt satellites $^1J_{Pt-P} \sim 3000$ Hz.

Cage 6

Clathrochelate **3** (5.20 mg, 6 μmol) and (dppp)Pd(OTf)$_2$ (10.45 mg, 13 μmol) were suspended in CH_3CN (4 mL) and the reaction mixture was stirred at 50 °C over night. The solution became clear after approximately 10 min. The solution was filtered using *Whatman* glass filters and the product was precipitated with Et_2O (40 mL). The product was isolated by filtration, washed with Et_2O (1 × 10mL), pentane (3 × 5mL) and dried under vacuum to give **6** in the form of an orange powder (13.73 mg, 1.3 μmol, 87%).

^{1}H NMR (600 MHz, CD_3CN) δ 8.76 (d, J = 5.8 Hz, 16H, CH_{ar}), 8.74 (d, J = 6.0 Hz, 16H, CH_{ar}), 7.78 (m, 32H, CH_{ar}), 7.66 (m, 24H, CH_{ar}), 7.63−7.47 (m, 64H, CH_{ar}), 7.48−7.28 (m, 96H, CH_{ar}), 3.21 (s, 32H, PCH_2), 3.16 (s, 16H, PCH_2CH_2), 2.08 (s, 72H, CH_3). Because of the poor solubility of **6**, a ^{13}C NMR spectrum was not recorded. ^{31}P NMR (162 MHz, CD_3CN) δ 8.80 (s), 8.74 (s).

Cage 7

Clathrochelate **4** (4.98 mg, 5 μmol) and (dppm)Pt(OTf)$_2$ (9.66 mg, 11 μmol) were suspended in CH_3CN (4 mL) and the reaction mixture was stirred at 50 °C over night. The solution became clear after approximately 30 min. The solution was filtered using *Whatman* glass filters and the product was precipitated with Et_2O (50 mL). The product was isolated by filtration, washed with Et_2O (1 × 10mL), pentane (3 × 5mL) and dried under vacuum to give **7** in the form of an orange powder (13.62 mg, 1.3 μmol, 97%).

^{1}H NMR (400 MHz, CD_3CN) δ 8.84 (two overlapping d, J = 6.8 Hz, 32H, CH_{ar}), 8.06 (s, 8H, CH_{ar}), 8.02−7.87 (m, 48H, CH_{ar}), 7.87−7.45 (m, 160H,CH_{ar}), 5.16 (t, J = 11.7 Hz, 16H, PCH_2), 2.60 (q, J = 7.4 Hz, 48H, CH_2CH_3), 0.87 (t, J = 7.5 Hz, 72H, CH_2CH_3). Because of the poor solubility of **7**, a ^{13}C NMR spectrum was not recorded. ^{31}P NMR (162 MHz, CD_3CN) δ –56.62 (s), –56.68 (s). ^{195}Pt satellites $^1J_{Pt-P} \sim 2800$ Hz.

3. NMR spectra

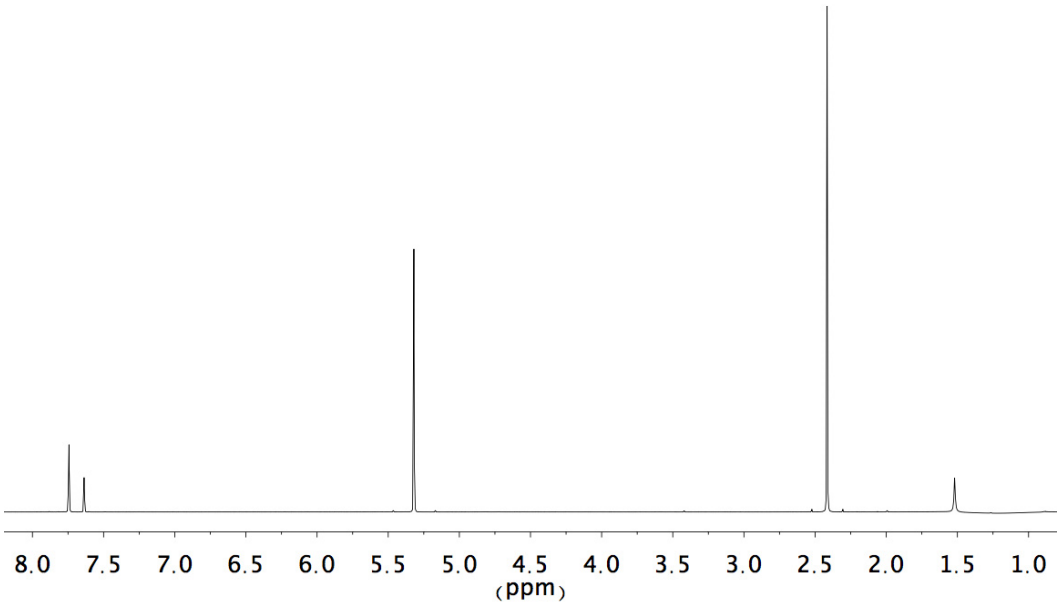

Figure S1. ^{1}H NMR spectrum of **1** recorded in CD_2Cl_2.

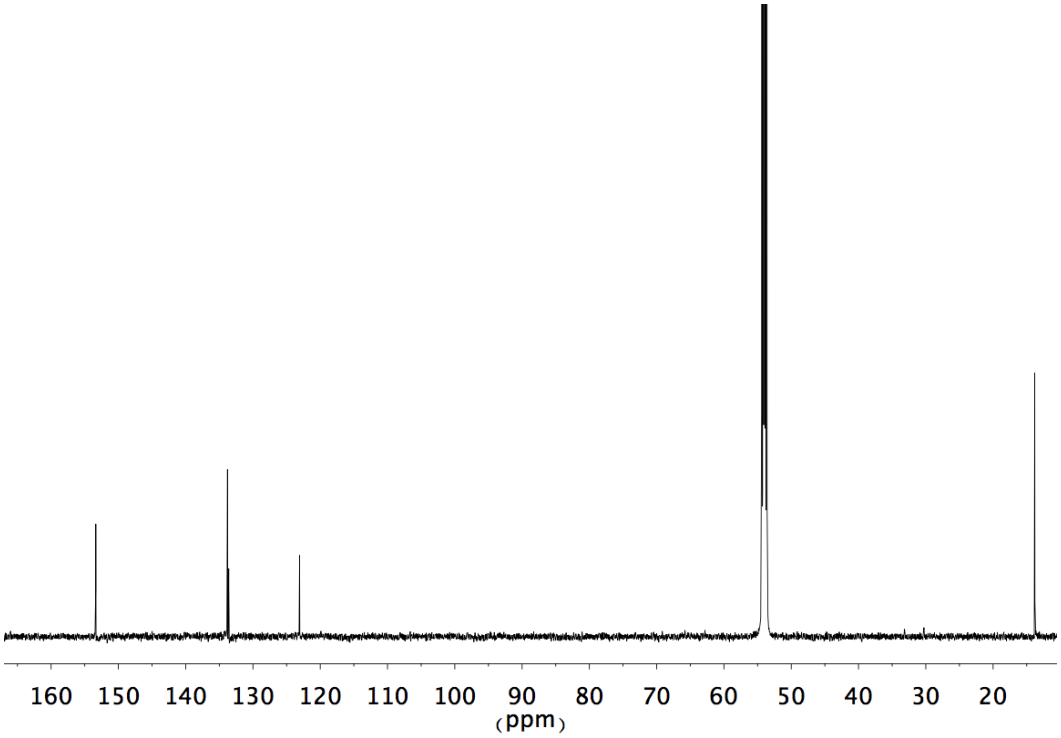

Figure S2. ^{13}C NMR spectrum of **1** recorded in CD_2Cl_2.

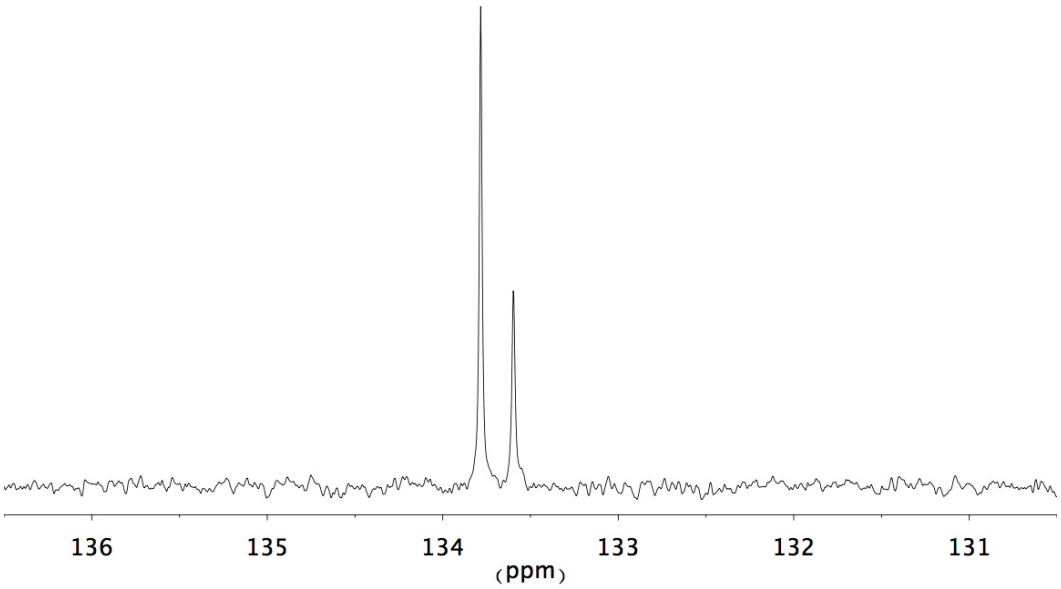

Figure S3. ^{13}C NMR zoom in spectrum of **1** recorded in CD_2Cl_2.

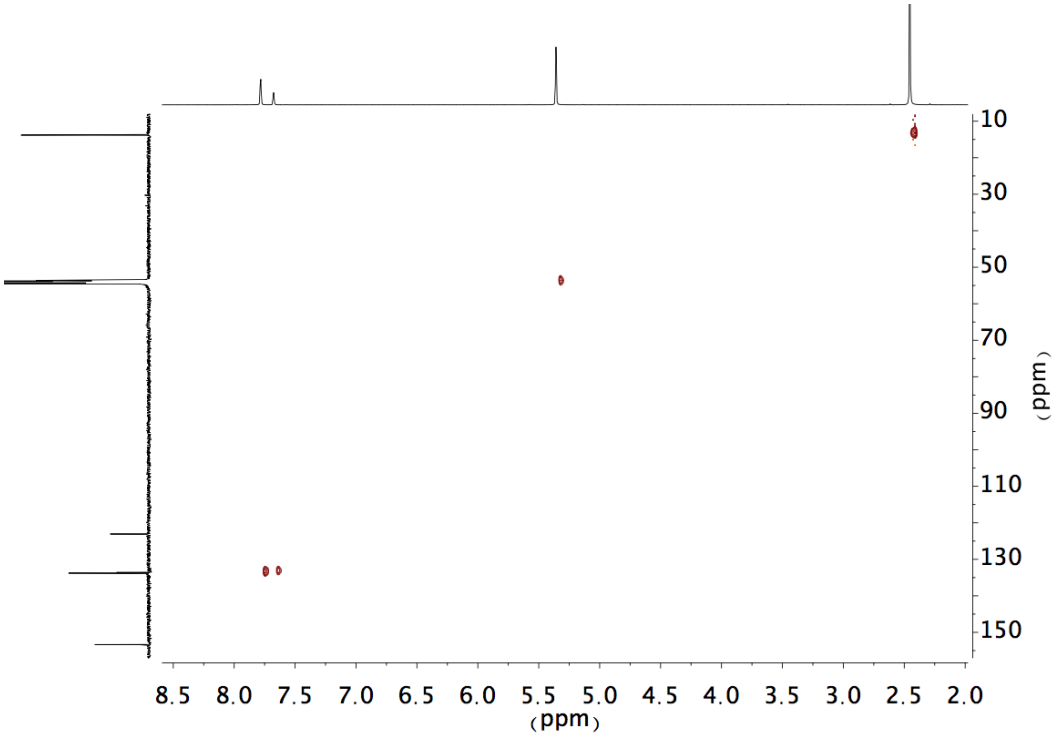

Figure S4. HSQC NMR spectrum of **1** recorded in CD_2Cl_2.

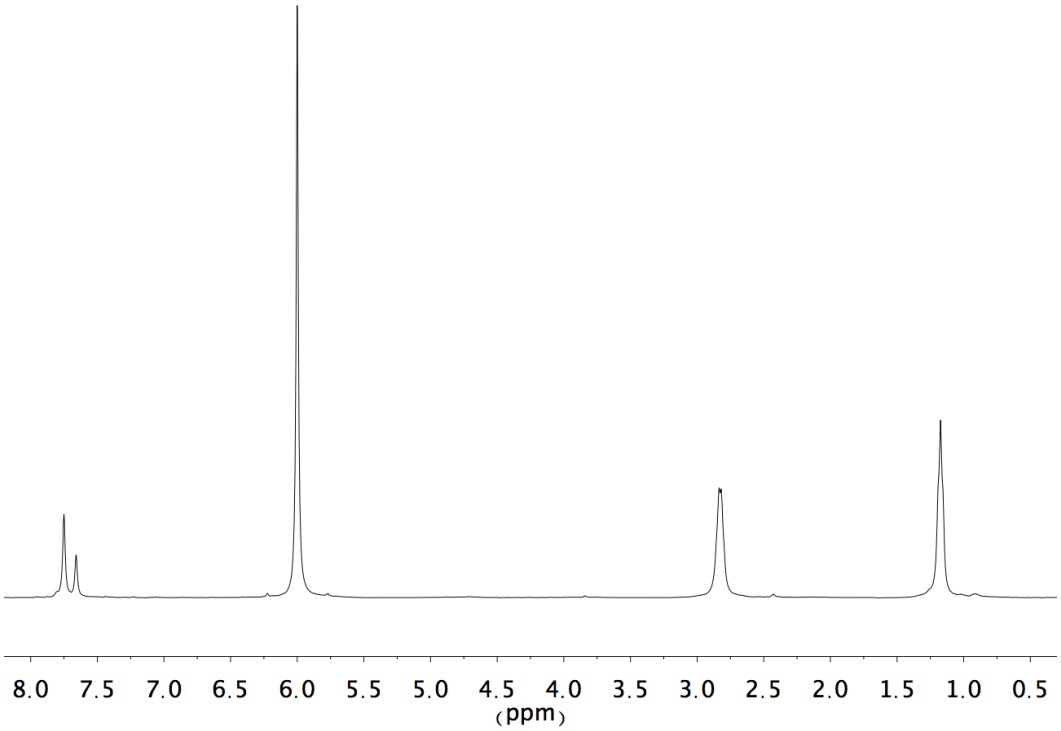

Figure S5. ^{1}H NMR spectrum of **2** recorded in $C_2D_2Cl_4$.

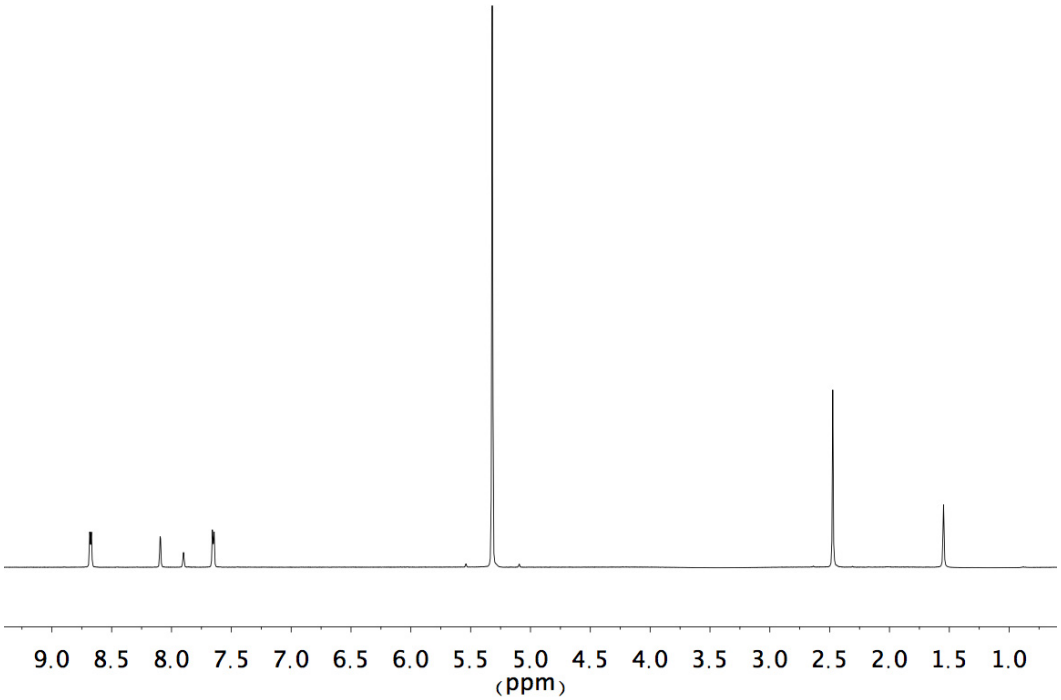

Figure S6. ^{1}H NMR spectrum of **3** recorded in CD_2Cl_2.

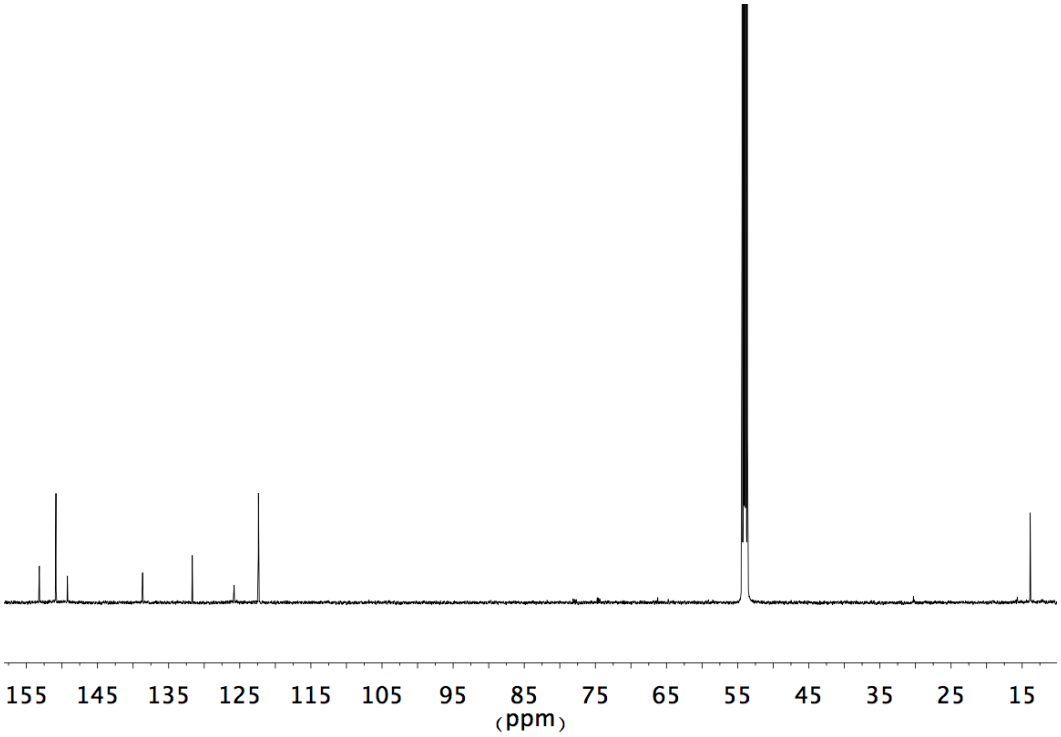

Figure S7. ^{13}C NMR spectrum of **3** recorded in CD_2Cl_2.

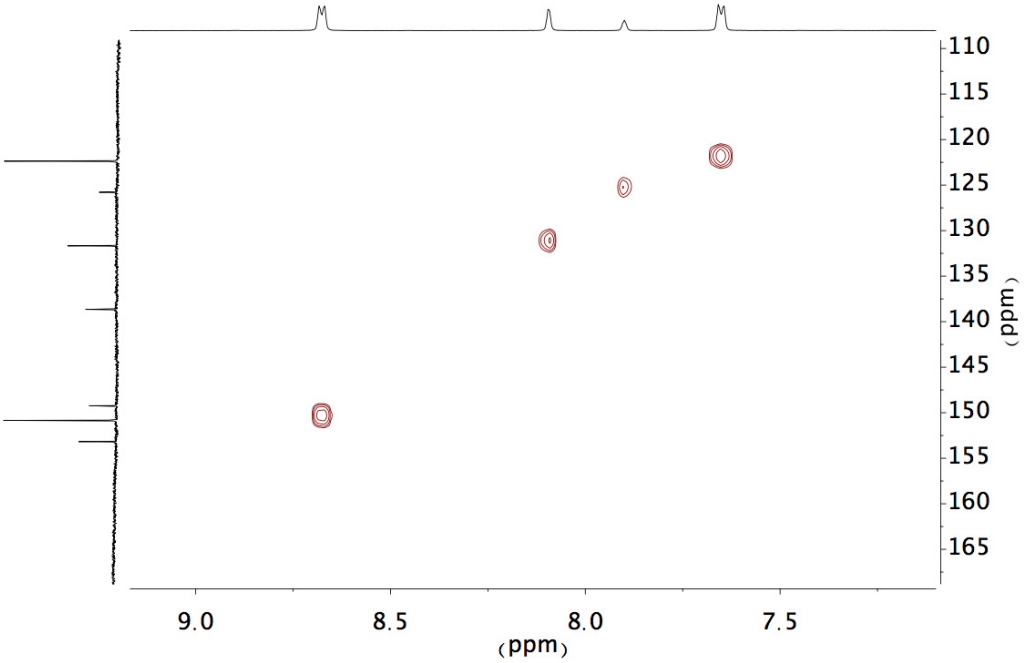

Figure S8. HSQC NMR spectrum aromatic region of **3** recorded in CD_2Cl_2.

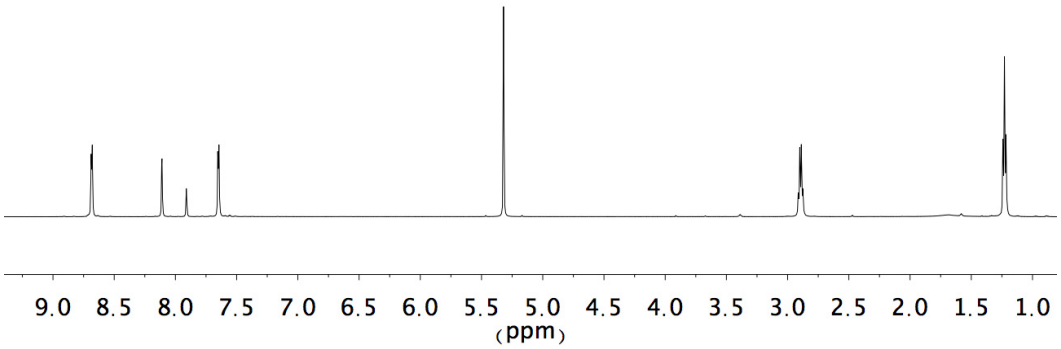

Figure S9. ^{1}H NMR spectrum of **4** recorded in CD_2Cl_2.

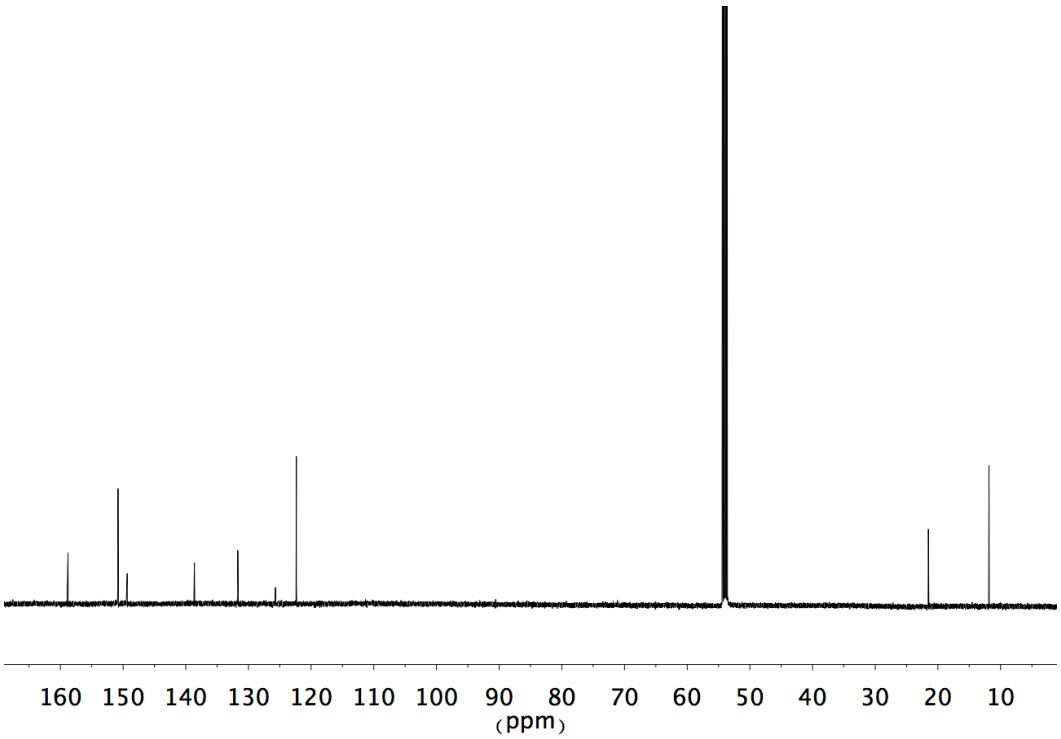

Figure S10. ^{13}C NMR spectrum of **4** recorded in CD_2Cl_2.

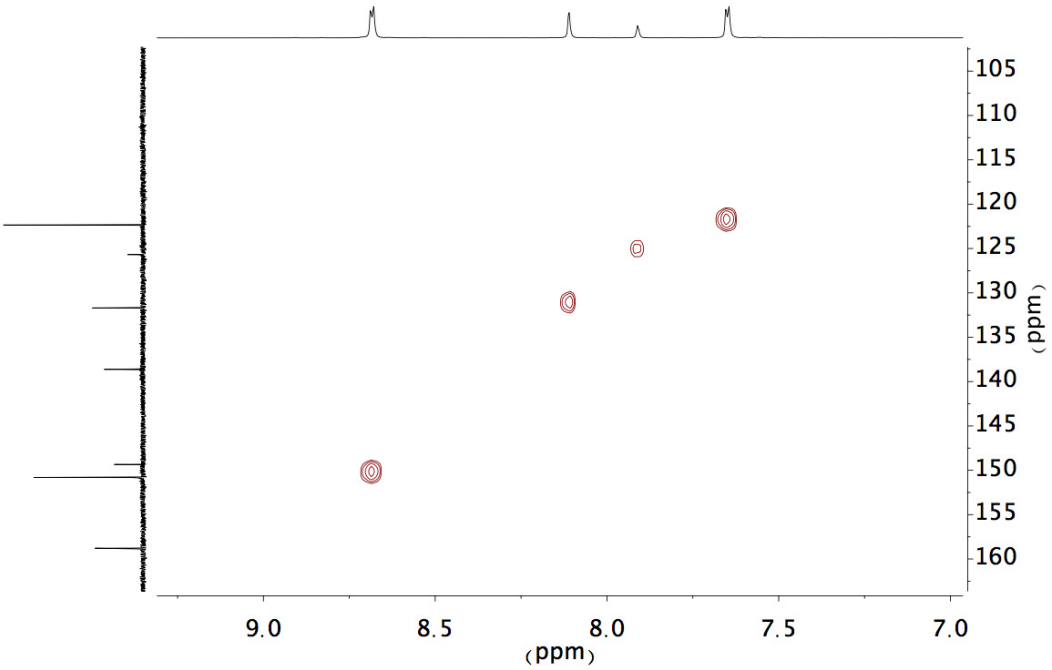

Figure S11. HSQC NMR spectrum aromatic region of **4** recorded in CD_2Cl_2.

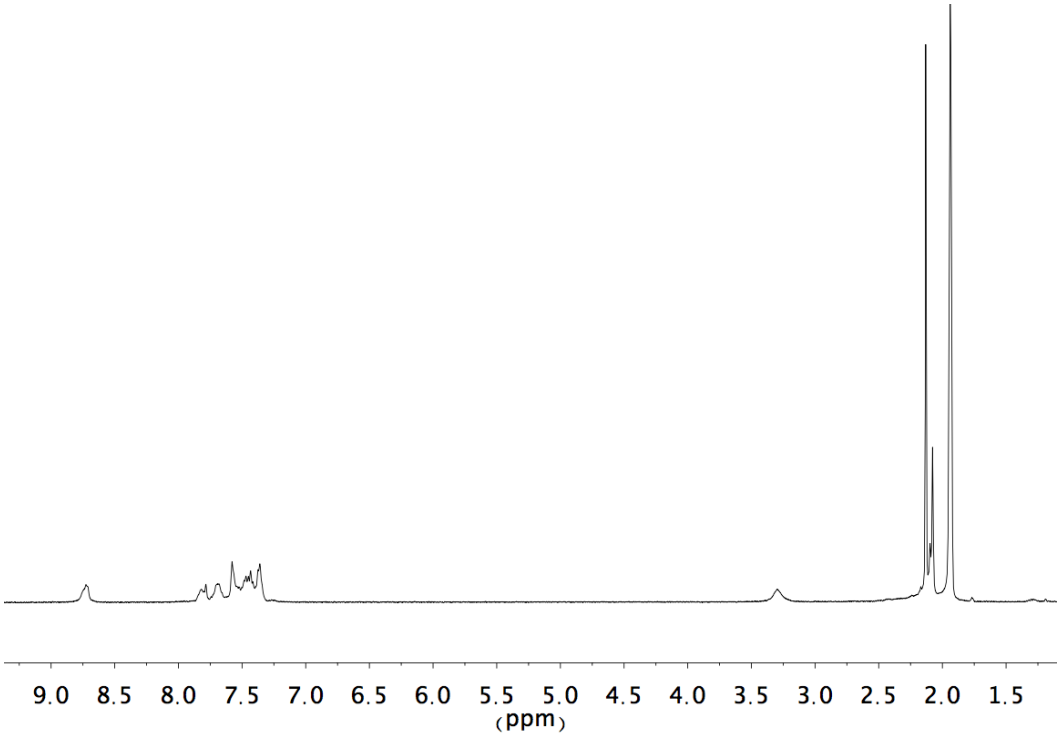

Figure S12. ^{1}H NMR spectrum of **5** recorded in CD_3CN.

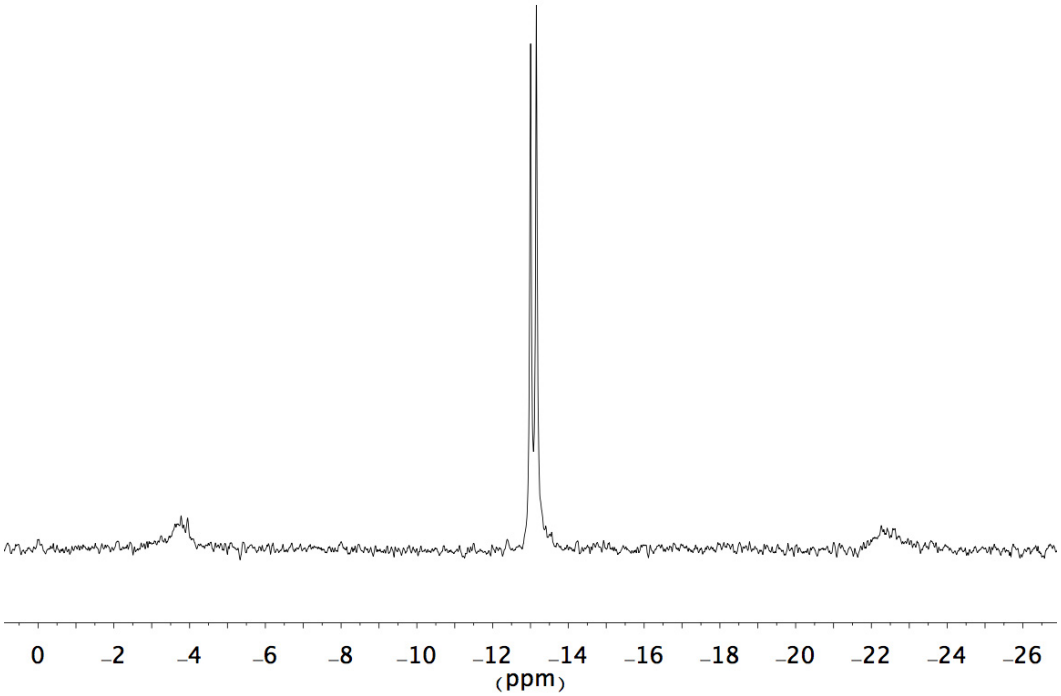

Figure S13. ^{31}P NMR spectrum of **5** recorded in CD_3CN.

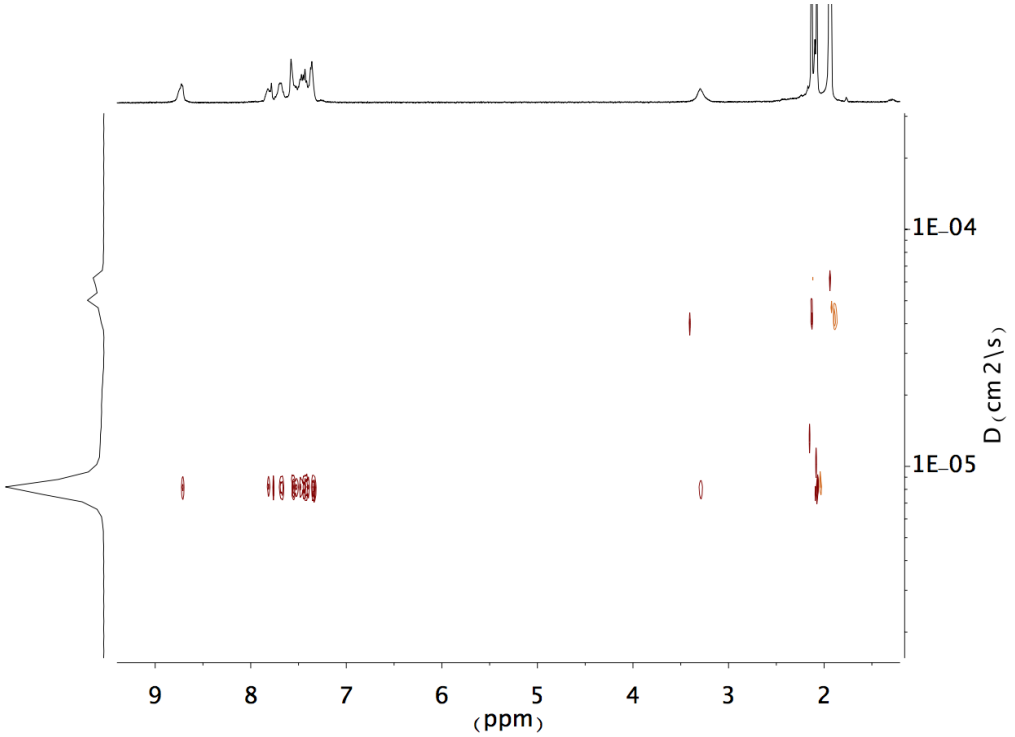

Figure S14. DOSY NMR spectrum of **5** recorded in CD_3CN.

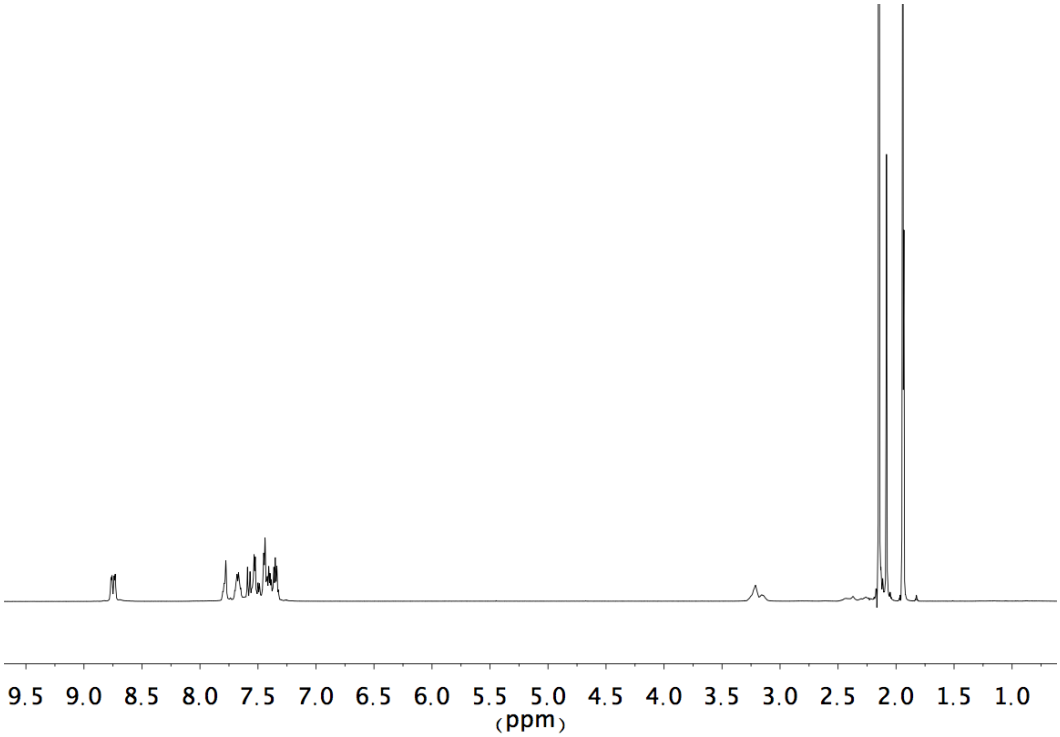

Figure S15. ^1H NMR spectrum of **6** recorded in CD_3CN.

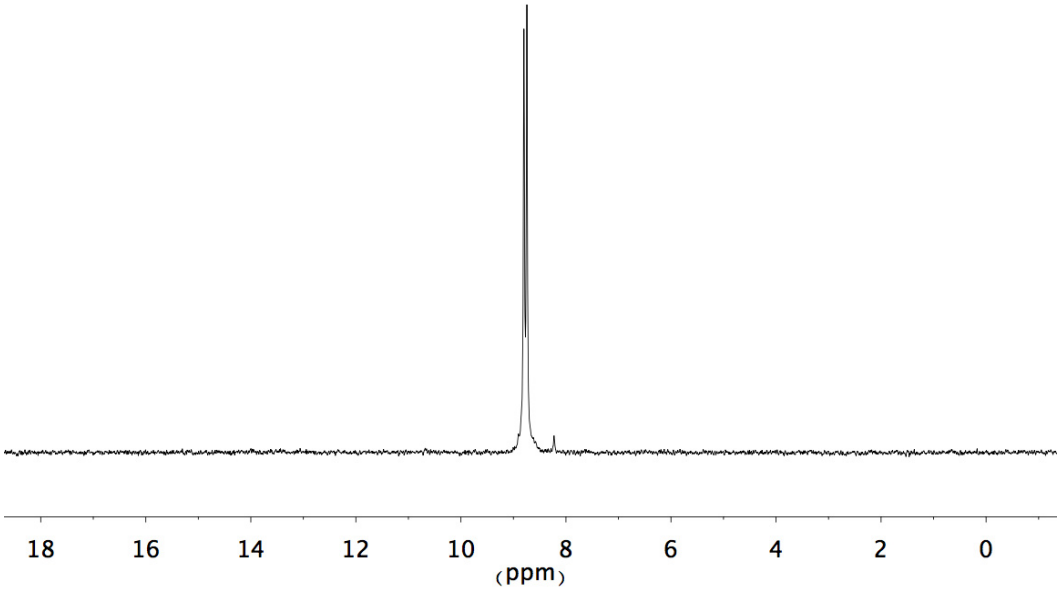

Figure S16. ^{31}P NMR spectrum of **6** recorded in CD_3CN.

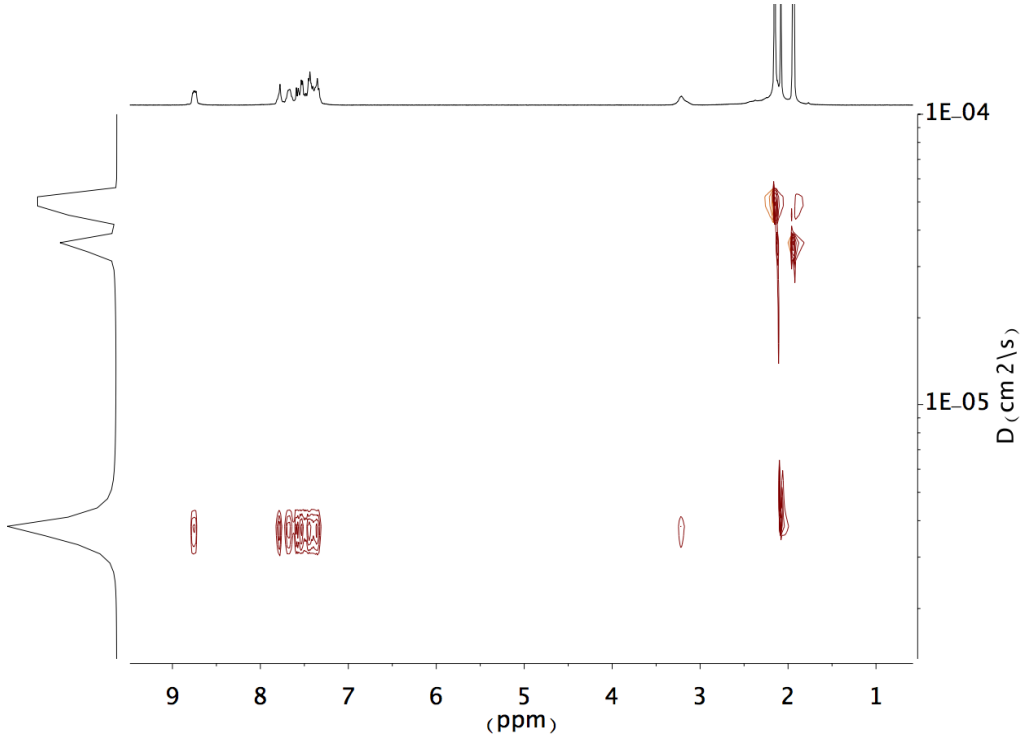

Figure S17. DOSY NMR spectrum of **6** recorded in CD_3CN.

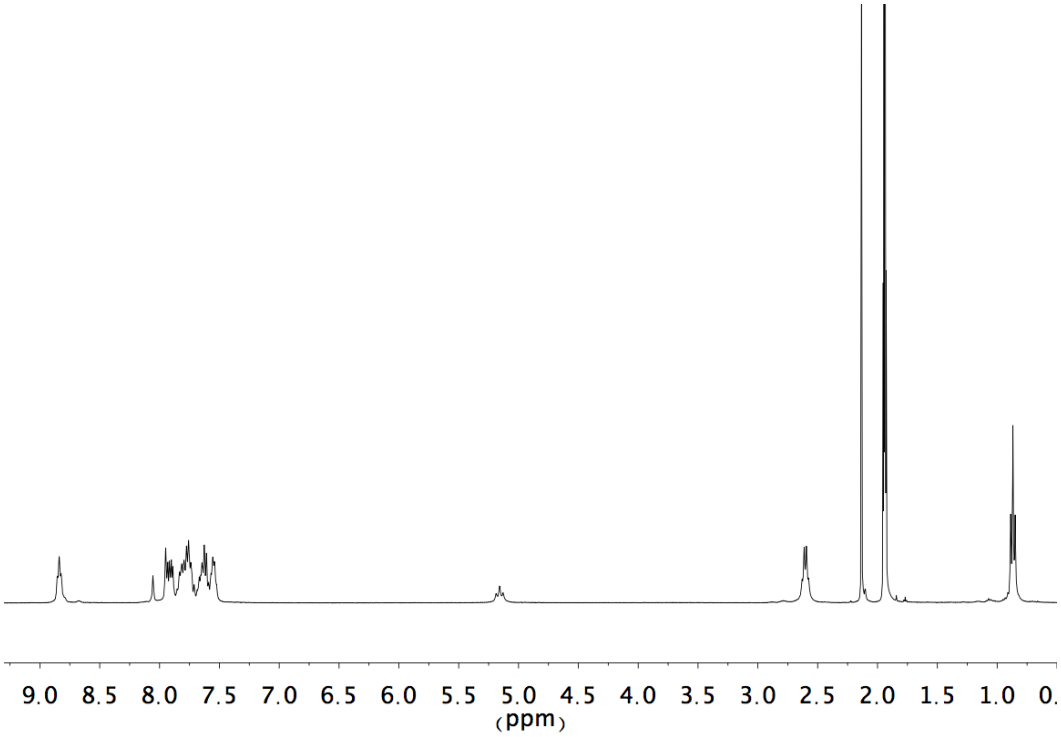

Figure S18. ^{1}H NMR spectrum of **7** recorded in CD_3CN.

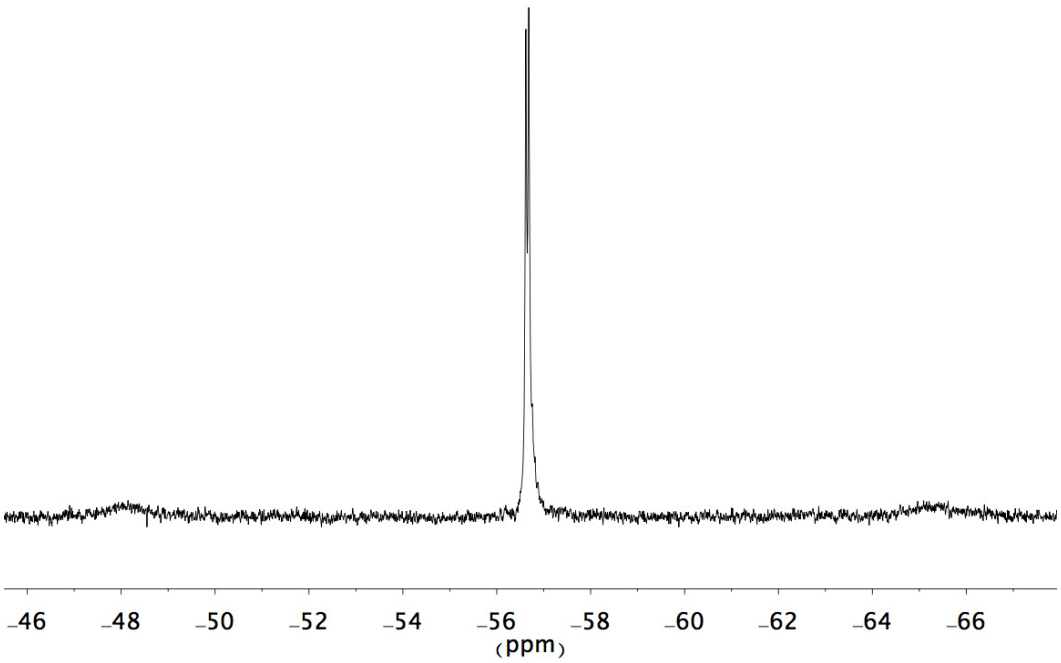

Figure S19. ^{31}P NMR spectrum of **7** recorded in CD_3CN.

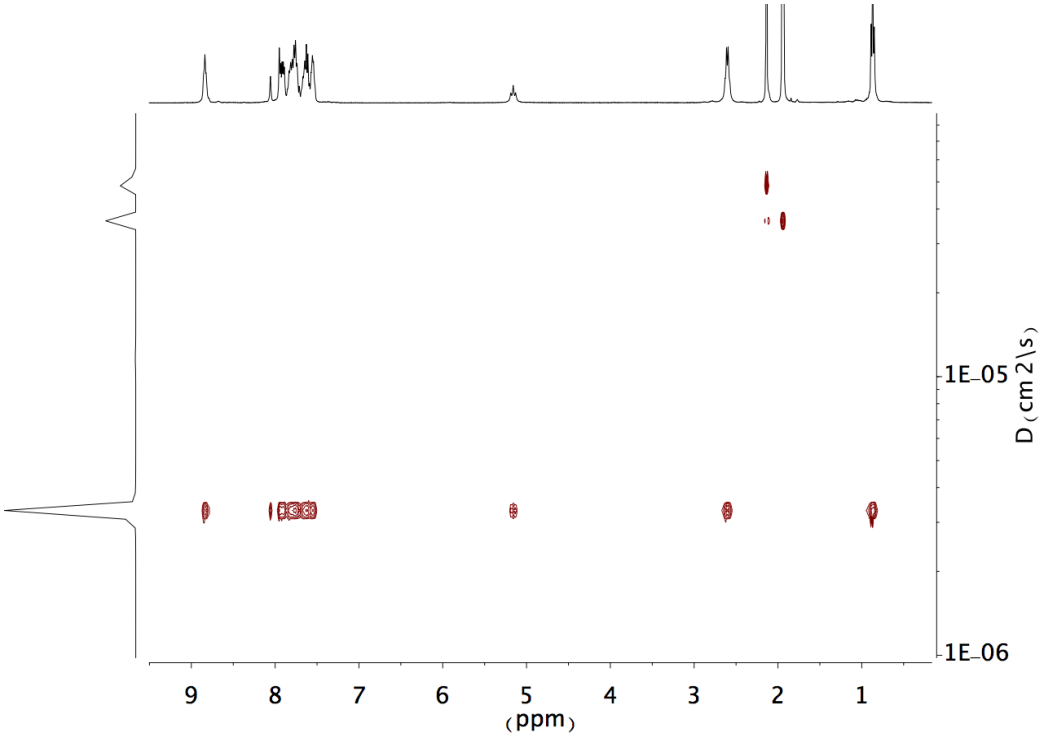

Figure S20. DOSY NMR spectrum of **7** recorded in CD_3CN.

4. Mass spectrometry

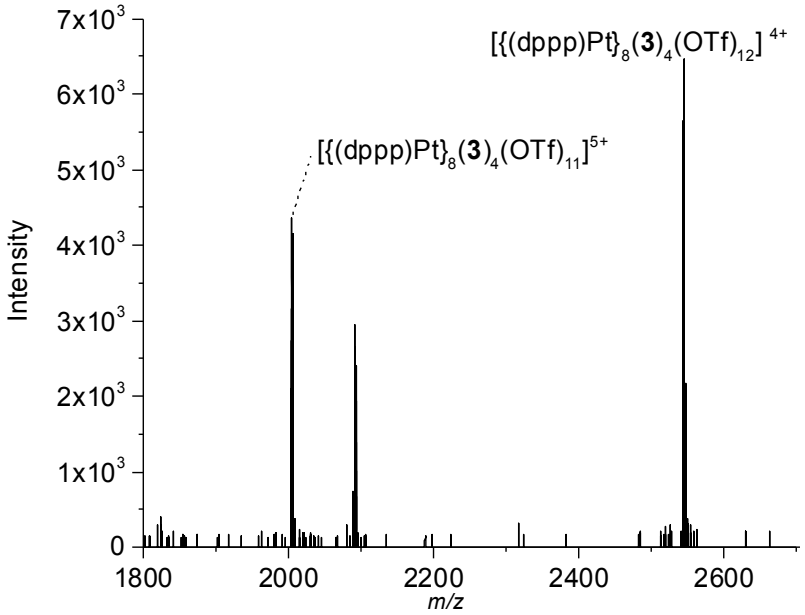

Figure S21. HRMS of cage **5**.

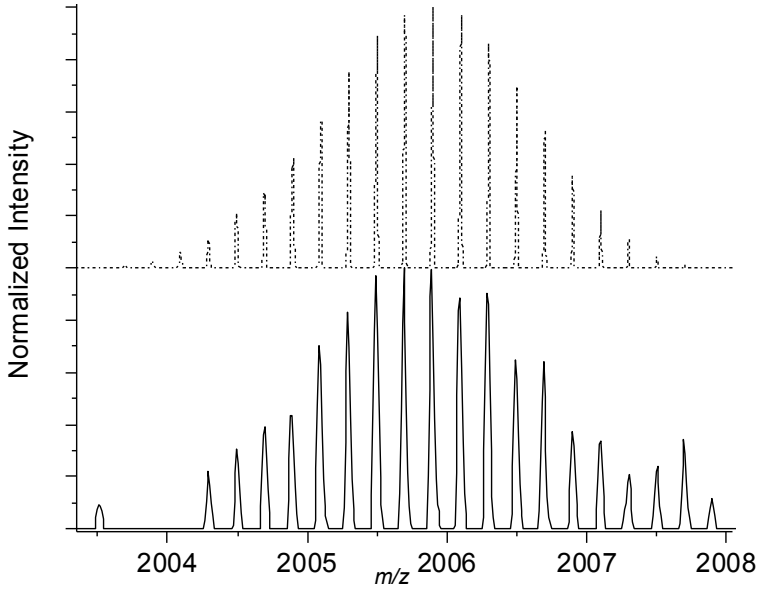

Figure S22. Zoom-in on the *m/z* distribution of cage **5** corresponding to $[\{(dppp)Pt\}_8(\mathbf{3})_4(OTf)_{11}]^{5+}$. *m/z* = 2004.89255 (bottom) and simulation (top).

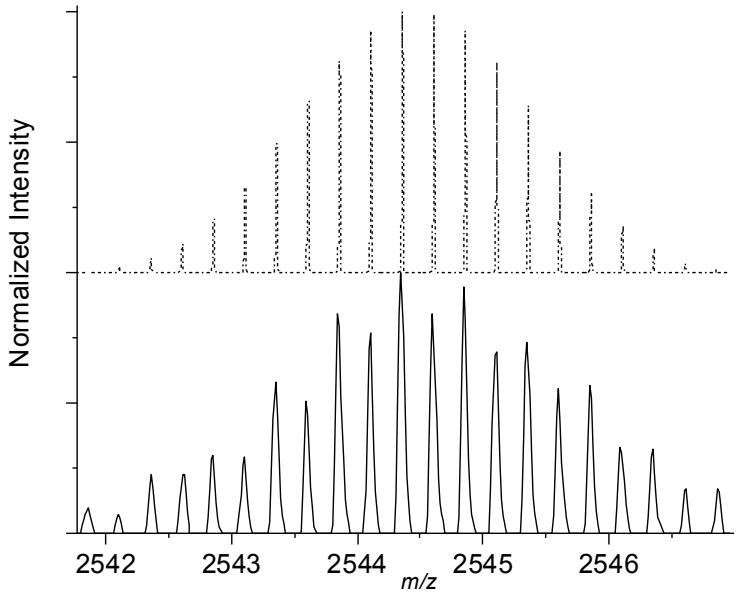

Figure S23. Zoom-in on the *m/z* distribution of cage **5** corresponding to $[\{(dppp)Pt\}_8(\mathbf{3})_4(OTf)_{12}]^{4+}$. *m/z* = 2543.353843 (bottom) and simulation (top). The difference between the simulated and the experimental spectra points to the presence of small amounts of a 2+ complex with the same *m/z ratio.*

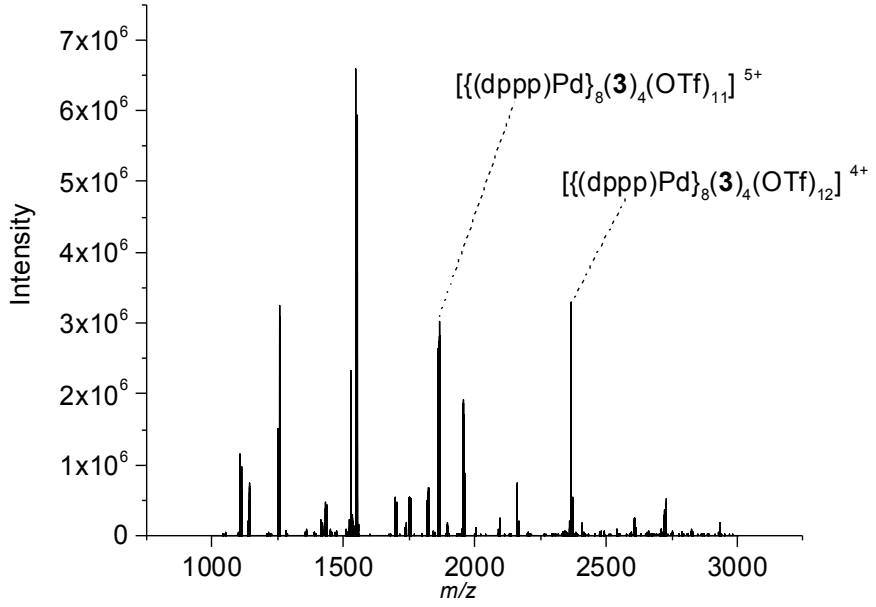

Figure S24. HRMS of cage **6**.

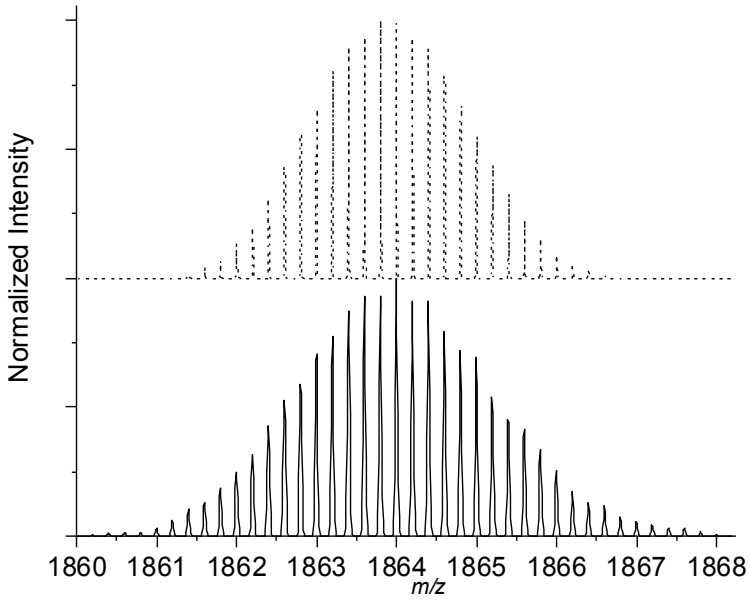

Figure S25. Zoom-in on the *m/z* distribution of cage **6** corresponding to $[\{(dppp)Pd\}_8(\mathbf{3})_4(OTf)_{11}]^{5+}$. *m/z* = 1862.3944 (bottom) and simulation (top).

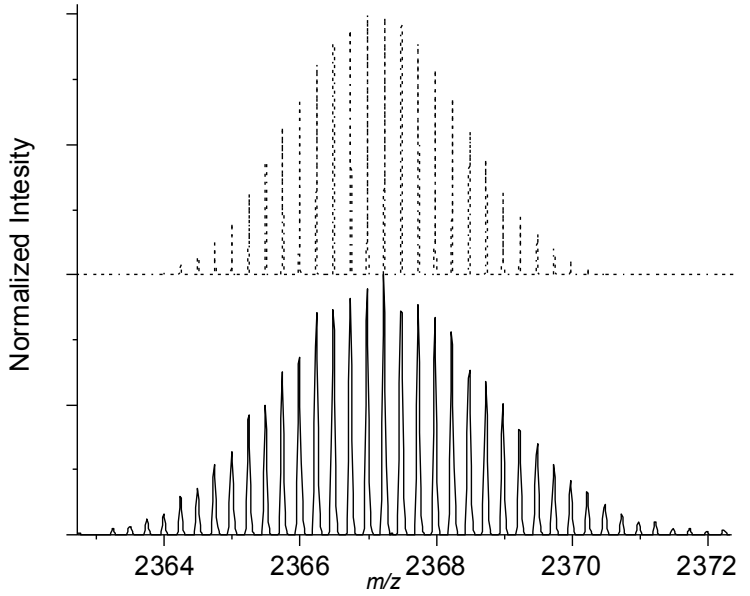

Figure S26. Zoom-in on the *m/z* distribution of cage **6** corresponding to $[\{(dppp)Pd\}_8(\mathbf{3})_4(OTf)_{12}]^{4+}$. *m/z* = 2365.2312 (bottom) and simulation (top).

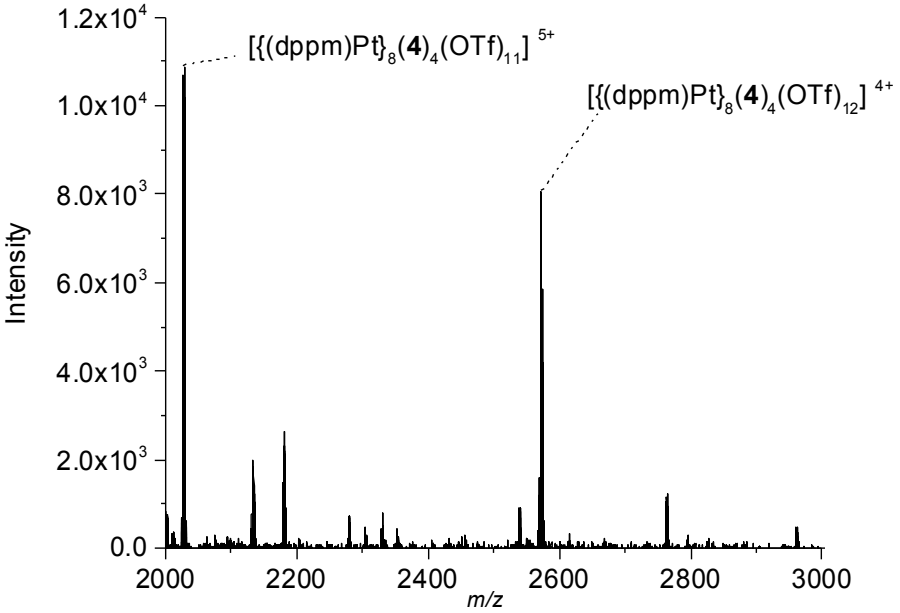

Figure S27. HRMS of cage **7** (*m/z* range 2000-3000).

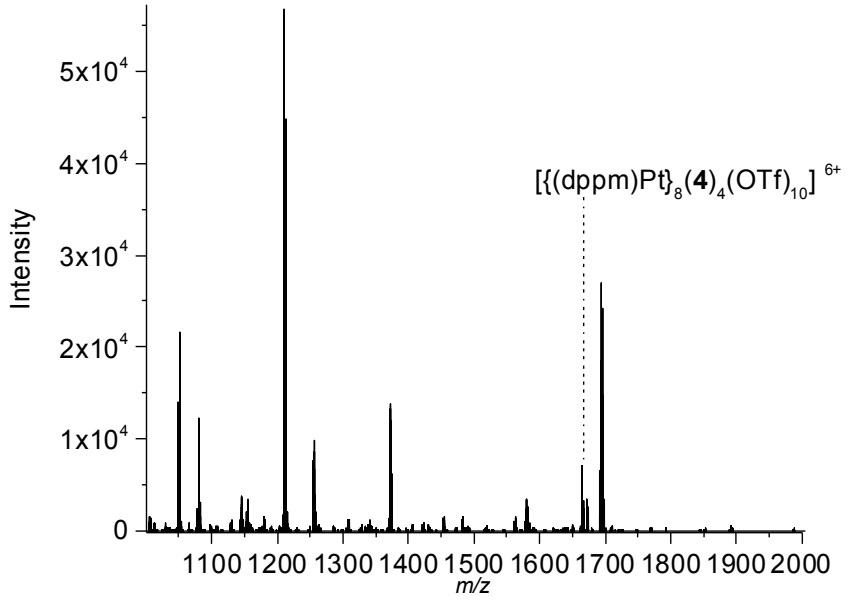

Figure S28. HRMS of **7** recorded in CH_3CN (*m/z* range 1000-2000).

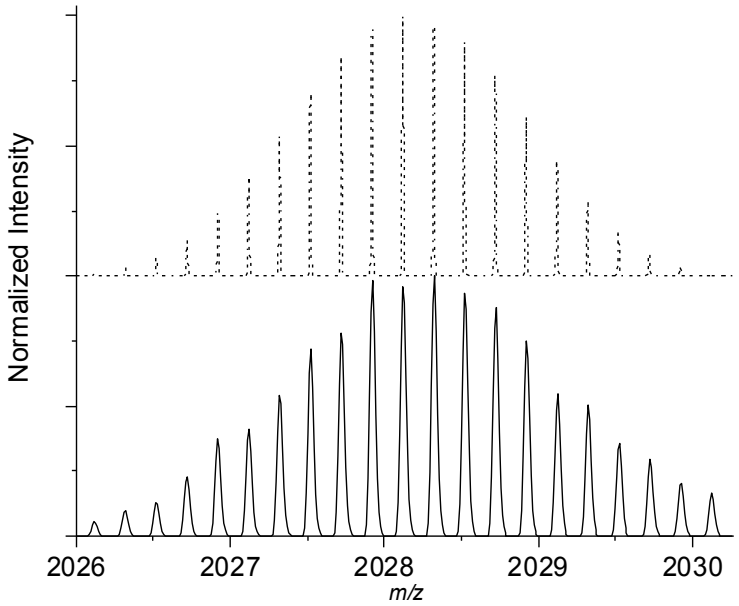

Figure S29. Zoom-in on the *m/z* distribution of cage **7** corresponding to $[\{(dppm)Pt\}_8(\mathbf{3})_4(OTf)_{11}]^{5+}$. *m/z* = 2027.31759 (bottom) and simulation (top).

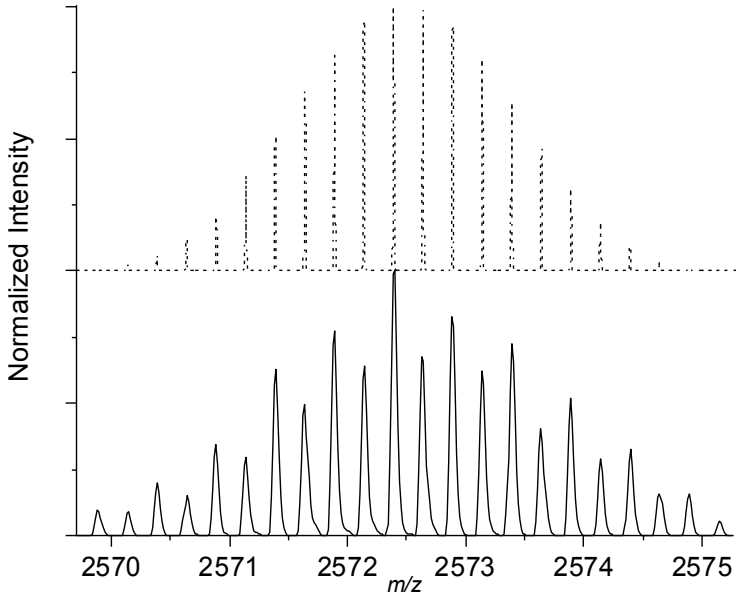

Figure S30. Zoom-in on the *m/z* distribution of cage **7** corresponding to $[\{(dppm)Pt\}_8(\mathbf{3})_4(OTf)_{12}]^{4+}$. *m/z* = 2571.38513 (bottom) and simulation (top). The difference between the simulated and the experimental spectra points to the presence of small amounts of a 2+ complex with the same *m/z ratio.*

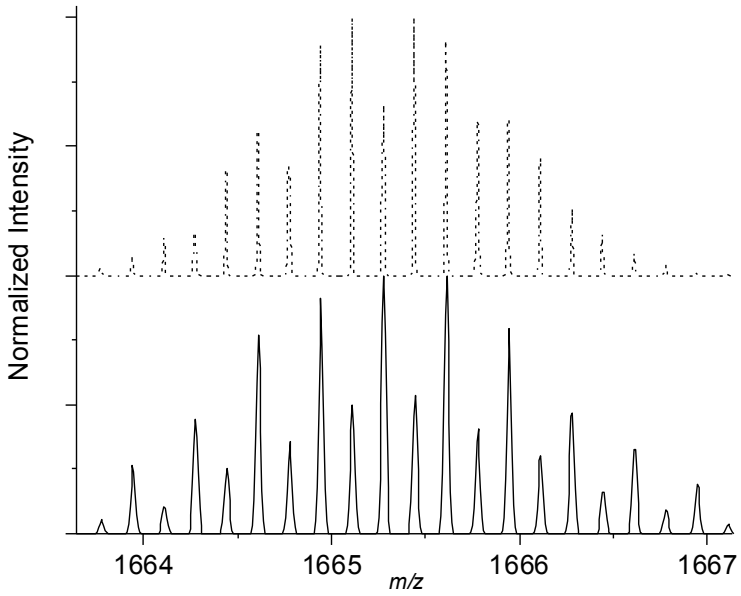

Figure S31. Zoom-in on the *m/z* distribution of cage **7** corresponding to $[\{(dppm)Pt\}_8(\mathbf{3})_4(OTf)_{10}]^{6+}$. *m*/*z* = 1664.6059 (bottom) and simulation (top). The difference between the simulated and the experimental spectra points to the presence of a 3+ complex with the same *m*/*z ratio*.

5. Geometrical considerations

The Pt atoms of complex **5** adopt a gyrobifastigium-like geometry in which the four triangular faces are approximate isosceles right triangles with two short sides **a** and a long side **b** (for an ideal gyrobifastigium, the triangular faces are equilateral triangles). The clathrochelate-based metalloligands panel the four rectangular faces, which have the dimensions **a** × **b**. The Fe atoms sit approximately at the center of the rectangular faces. The gyrobifastigium-like geometry can be described as two face-sharing trigonal prisms. If we rotate the lower prism with respect to the upper prims by 90°, we end up with a square prismatic structure of the dimensions **a** × **a** × **b** (Figure S32). Square prismatic structures are more commonly observed for $M^{II}_8L_4$-type coordination cages.

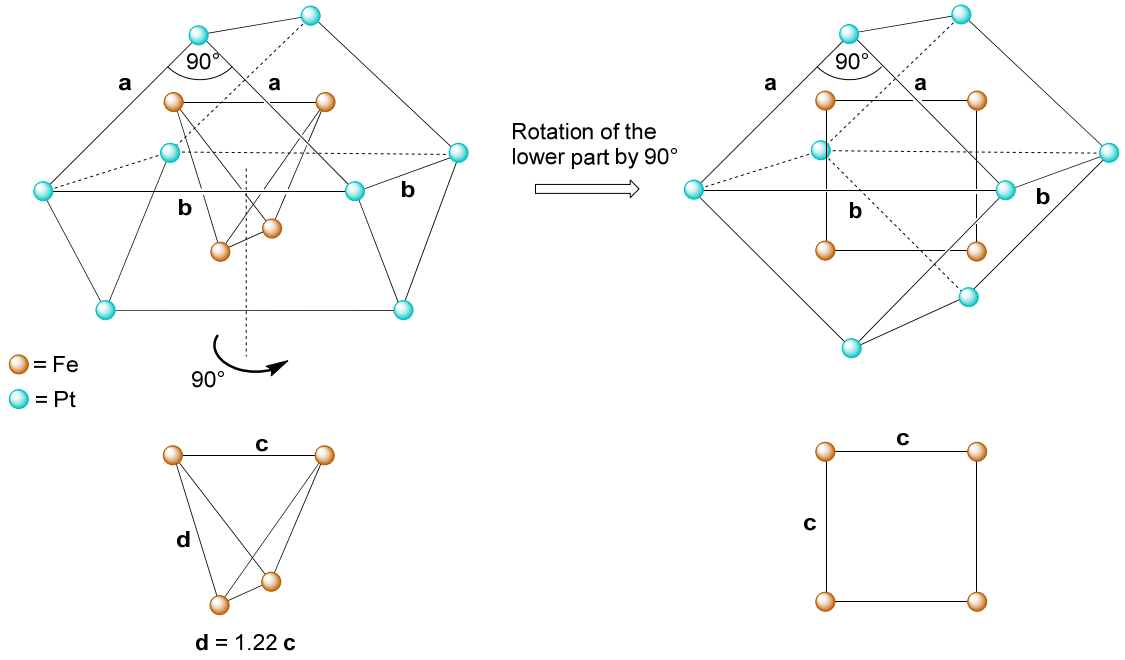

Figure S32. A distorted gyrobifastigium with isosceles right triangles as triangular faces can be converted into a square prism by rotation of the lower part with respect to the upper part by 90°.

For the gyrobifastigium-like geometry, the Fe atoms adopt a distorted tetrahedral geometry with two short edges **a** and four long edges **d**. For the square prismatic structure, the Fe atoms describe a square of the dimensions **c** × **c**. Assuming idealized structures as depicted in Figure S32, one can calculate that $\mathbf{d} = (1.5)^{1/2} \times \mathbf{c}$, that is **d** is around 1.22 times longer than **c**. These calculated values match quite nicely what is observed for complex **5**, with the average long Fe···Fe distance (12.3 Å) being 1.24 times longer than the average short Fe···Fe distance (9.9 Å). In a hypothetical square prism, one would observe four short Fe···Fe contacts instead of just two for the gyrobifastigium-like structure. Considering the substantial lateral size of the Fe-centered clathrochelate complexes, the formation of a square prism is probably disfavoured due to steric interactions between the clathrochelates.

6. Single crystal X-ray analysis

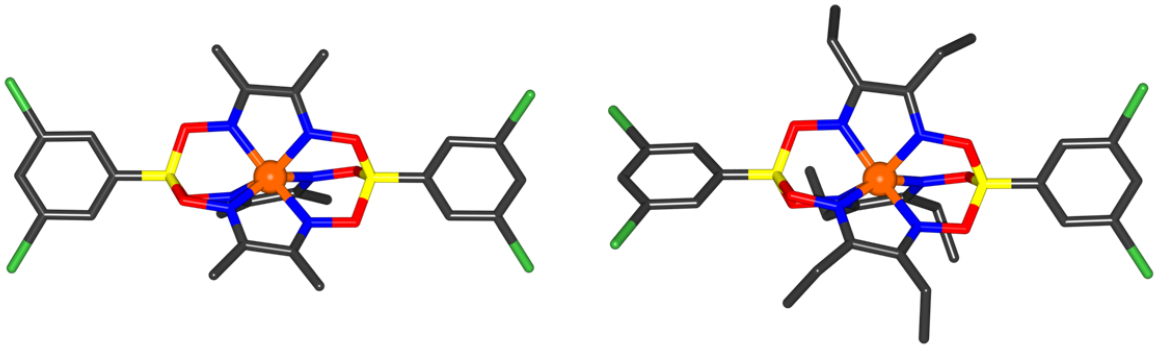

Figure S33. Molecular structures of clathrochelate **1** (left) and **2** (right) as determined by X-ray crystallography. Color coding: C: gray, B: yellow, Fe: orange, N: blue, O: red, Br: green. Hydrogen atoms are omitted for clarity.

Crystallization methods: Clathrochelate **1**: Slow diffusion of Et_2O into a solution of **1** in DCM. Clathrochelate **2**: Slow diffusion of Et_2O into a solution of **2** in TCE. Clathrochelate **4**: Slow evaporation of a solution of the ligand in DCM. Cage **5**: Slow diffusion of Et_2O into a solution of the cage in CH_3CN.

Intensity data for clathrochelate **1** was measured at low temperature [140(2) K] using Cu α radiation on a RigakuSuperNova dual system equipped with an Atlas CCD detector. The datasets were reduced and corrected for absorption with CrysAlis Pro.[6] Disordered solvent molecules were treated with solvent mask procedure.[7]

Intensity data for clathrochelate **2** was measured at low temperature [120(2) K] using Mo α radiation on a Bruker APEX II CCD diffractometer equipped with a kappa geometry goniometer. The datasets were reduced by EvalCCD[8] and than corrected for absorption by SADABS.[9]

Intensity data for clathrochelate **3** was measured at low temperature [140 (2) K] using Cu α radiation on a RigakuSuperNova dual system equipped with an Atlas CCD detector. The datasets were reduced and than corrected for absorption by CrysAlis Pro.[6] Solvent molecules too disordered to be modelled were treated using SQUEEZE procedure.[10]

Intensity data for clathrochelate **4** was measured at low temperature [100 (1) K] using Cu α radiation on a RigakuSuperNova dual system equipped with an Atlas CCD detector. The datasets were reduced and than corrected for absorption by CrysAlis Pro.[6]

Intensity data for cage **5** were measured at low temperature [140.0(1) K] using Cu α radiation on a RigakuSuperNova dual system equipped with an Atlas CCD detector. The datasets were reduced and then corrected for absorption by CrysAlis Pro.[6]

Intensity data for cage **5** were measured at low temperature [140.0(1) K] using Cu α radiation on a RigakuSuperNova dual system equipped with an Atlas CCD detector. The datasets were reduced and then corrected for absorption by CrysAlis Pro.[6]

The asymmetric unit is composed by a full cage **5**, consisting of 8 $[Pt(Ph_2P(CH_2)_3PPh_2)]^{2+}$ complexes and 4 Fe complexes **3**, and 16 triflate counterions. In the final refinement, hydrogen atoms were included at calculated positions. Platinum, iron, phosphorous and sulphur atoms were treated anisotropically, while all other non-hydrogen atoms were treated isotropically. Planarity restrains were applied to aromatic groups and to the dimethylglyoxime residues, using the card FLAT of SHELX.[11] Bond lengths and angles were restrained for the dimethylglyoxime residues and for the triflate counterions, using the cards DFIX, DANG and SAME.[11] Restrains were also applied on the thermal parameters of the atoms (card SIMU). Solvent molecules were too disordered to be modelled, but their contribution was taken into account using the SQUEEZE/PLATON procedure.[10] The residual electron density of 2481 electrons/cell where found in the voids of the crystal (corresponding to about 42% of the cell volume). A refinement using reflections modified by the SQUEEZE[10] procedure behaved well and the R-factor [$I>2\sigma(i)$] was reduced from 0.24 to 0.17.

All the structures were solved and refined with SHELX.[11] All graphics were produced with Olex2.[7]

Crystallographic data have been deposited to the CCDC and correspond to the following codes: **1** (1492928), **2** (1492925), **3** (1495320), **4** (1492926), **5** (1492927). Copies of the data can be obtained free of charge on application to the CCDC, 12 Union Road, Cambridge, CB2 1EZ, U.K. (fax, (internat.) +44-1223-336033; E-mail, deposit@ccdc.cam.ac.uk)

Complex	**1**	**2**	**3**
Empirical formula	$C_{24}H_{24}B_2N_6O_6FeBr_4$	$C_{30}H_{36}B_2N_6O_6FeBr_4$	$C_{44}H_{40}B_2N_{10}O_6Fe$
Mol. Weight / g mol^{-1}	889.60	973.76	882.33
Crystal size / mm^3	0.210 × 0.194 × 0.146	0.337 × 0.168 × 0.158	0.294 × 0.264 × 0.054
Crystal system	Monoclinic	Monoclinic	Monoclinic
Space group	*I*2/*a*	*C*2/*c*	$P2_1/c$
a / Å	14.7088(4)	26.140(4)	9.4866(4)
b / Å	12.8848(3)	8.4019(12)	10.6979(3)
c / Å	18.6454(6)	18.4972(13)	47.959(2)
α / °	90	90	90
β / °	102.859(3)	117.658(7)	94.425(5)
γ / °	90	90	90
Volume / $Å^3$	3445.02(15)	3598.2(8)	4852.7(3)
Z	4	4	4
Density g/cm^{-3}	1.715	1.798	1.208
Temperature / *K*	140(2)	120(2)	140.0(1)
Absorption Coeff. / mm^{-1}	9.326	4.912	2.936
2Θ range / °	6.95 to 152.2312	5.158 to 54.994	7.396 to 151.222
Index ranges	-18 ≤ h ≤ 18, -15 ≤ k ≤ 16, -23 ≤ l ≤ 23	-33 ≤ h ≤ 33, -10 ≤ k ≤ 10, -23 ≤ l ≤ 24	-11 ≤ h ≤ 8, -13 ≤ k ≤ 13, -59 ≤ l ≤ 58
Reflections collected	12880	23401	34528
Independent reflections	3554 (R_{int} = 0.0252)	4117 (R_{int} = 0.07107)	9908 (R_{int} = 0.0614)
Absorption correction	Gaussian	Multi-scan	Semi-empirical from equivalents
Max. & min. transmission	0.427 and 0.247	0.7456 and 0.3947	0.42183 and 1.000
Data / restraints / param.	3554/0/198	4117 / 0 / 225	9908 / 0 / 605
Goodness-of-fit on F^2	1.043	1.119	1.082
Final *R* indices [I > 2 s (I)]	*R1* = 0.0429, wR_2 = 0.1005	*R1* = 0.0442, w*R2* = 0.0834	*R1* = 0.0807, w*R2* = 0.1791
R indices (all data)	*R1* = 0.0439, w*R2* = 0.1010	*R1* = 0.0700, w*R2* = 0.0931	*R1* = 0.0869, w*R2* = 0.1824
Larg. diff. peak/hole / e$Å^{-3}$	0.973 and -1.233	0.67 and -0.51	1.076 and -0.722

Table S1 Crystallographic data for **1**, **2** and **3**.

Complex	**4**	**5**
Empirical formula	$C_{50}H_{52}B_2N_{10}O_6Fe$	$C_{408}H_{368}B_8F_{48}Fe_4N_{40}O_{72}P_{16}Pt_8S_{16}$
Mol. Weight / g mol^{-1}	966.48	10774.48
Crystal size / mm^3	0.698 × 0.291 × 0.214	0.322 × 0.148 × 0.036
Crystal system	Monoclinic	Triclinic
Space group	$P2_1/c$	*P-1*
a / Å	8.84673(5)	28.3614(16)
b / Å	38.91135(19)	28.8276(11)
c / Å	14.15673(7)	41.0379(16)
α / °	90	101.861(4)
β / °	105.3120(5)	92.914(4)
γ / °	90	104.120(4)
Volume / Å^3	4700.30(4)	31663(3)
Z	4	2
Density g/cm^{-3}	1.366	1.271
Temperature / *K*	100.0(1)	140.0(1)
Absorption Coeff. / mm^{-1}	3.078	6.051
2Θ range / °	7.892 to 150.566	6.702 to 103.216
Index ranges	-6 ≤ h ≤ 11, -48 ≤ k ≤ 45, -17 ≤ l ≤ 17	-28 ≤ h ≤ 28, -29 ≤ k ≤ 29, -0 ≤ l ≤ 41
Reflections collected	33734	67589
Independent reflections	9562 (R_{int} = 0.0229)	67589 (R_{int} = 0.1270)
Absorption correction	Gaussian	Gaussian
Max. & min. transmission	0.622 and 0.314	0.824 and 0.314
Data / restraints / param.	9562 / 0 / 629	67589 / 9293 / 2775
Goodness-of-fit on F^2	1.049	1.022
Final *R* indices [I > 2 s (I)]	*R1* = 0.0299, w*R2* = 0.0785	*R1* = 0.1667, w*R2* = 0.3590
R indices (all data)	*R1* = 0.0310, w*R2* = 0.0794	*R1* = 0.2662, w*R2* = 0.4339
Larg. diff. peak/hole / eÅ^{-3}	0.37 and -0.32	1.36 and -1.35

Table S2 Crystallographic data for **4** and **5**.

7. References

(1) A. B. Zaitsev, E. Y. Schmidt, A. M. Vasil'tsov, A. I. Mikhaleva, O. V. Petrova, A. V. Afonin, and N. V. Zorina, *Chem. Heterocycl. Compd.*, 2006, **42**, 34.

(2) N. C. Dopke and H. E. Oemke, *Inorg. Chim. Acta,* 2011, **376**, 638.

(3) P. J. Stang,D. H. Cao, S. Saito and A. M. Arif, *J. Am. Chem. Soc.*, 1995, **117**, 6273.

(4) C. E. Housecroft, B. A. M. Shaykh, A. L. Rheingold and B. S. Haggerty, *Inorg. Chem.*, 1991, **30**, 125.

(5) L. Patiny and A. Borel, *J. Chem. Inf. Model.*, 2013, **53**, 1223.

(6) CrysAlis PRO, 2009–2014, Agilent Technologies Ltd, Yarton, Oxfordshire, UK.

(7) O. V. Dolomanov, L. J. Bourhis, R. J. Gildea, J. A. K. Howard and H. Puschmann, *J. Appl. Cryst.,* 2009, **42**, 339.

(8) A. J. M. Duisenberg, L. M. J. Kroon-Batenburg and A. M. M. Schreurs, *J. Appl. Cryst.*, 2003, **36**, 220.

(9) Bruker-Nonius, APEX, SAINT, SADABS and XPREP, Bruker AXS Inc., Madison, Wisconsin, USA, 2013.

(10) A. L. Spek, *Acta Cryst*. *D*, 2009, **65**, 148.

(11) G. M. Sheldrick, *Acta Cryst. C*, 2015, **71**, 3.